MACRO POROSITY FORMATION: A STUDY IN HIGH PRESSURE DIE CASTING

David Blondheim Jr. and **Alex Monroe**
Mercury Marine – Mercury Castings, A Division of Brunswick, Inc., Fond du Lac, WI, USA

David Blondheim Jr.
Colorado State University, Fort Collins, CO, USA

Alex Monroe
Michigan Technological University, Houghton, MI, USA

Abstract

Porosity formation in high pressure die casting (HPDC) impacts mechanical properties and casting quality. Much is published regarding micro porosity and its impact on mechanical properties, but there is limited research on the actual formation of macro porosity. In production applications, macro porosity plays a critically important role in casting quality and acceptance by the customer. This paper argues that the most useful definition of macro porosity is the limits of visual detectability. With this definition, it will be shown macro porosity presents stochastically within a controlled HPDC process. This means macro porosity has a random probability distribution or pattern that should be analyzed statistically and cannot be predicted precisely.

The general region where macro porosity forms is predictable with simulation, but its actual size and distribution of the voids are random. These results challenge the industry accepted practices for inspections and process controls. This also underscores the importance of up-front design for manufacturability to avoid macro porosity-related quality issues.

Keywords: *high pressure die casting, porosity, casting defects, defect classification, macro porosity, micro porosity*

Introduction

Porosity is considered a defect, and it is inherent to aluminum high pressure die casting (HPDC) due to the nature of metal solidification.[1] Research completed by the North American Die Casting Association (NADCA) shows that porosity concerns are one of the leading contributors to scrap costs and the biggest problem within die casting.[2] Approximately 30% of the industry has identified addressing porosity as a top concern.[3] There is high motivation to improve porosity scrap given the die casting industry has $8 billion annual sales in North America[4] and suffers from an 8% median scrap rate.[5] Porosity defects can be described by the primary cause: shrink porosity and gas porosity and classified by the size: micro porosity and macro porosity.[6,7] The cause and size provide one high-level classification system for porosity, although more detailed defect classification systems exist.[2,8,9]

Porosity is well documented within the HPDC industry.[1,2,6,10,11] Shrink porosity is caused by volumetric contraction of metals during solidification. Shrink porosity is often irregular, with ragged shapes. Gas porosity occurs when a gas concentration within the liquid metal is higher than the solubility of the metal. Gas porosity is typically spherical in shape. The mechanisms causing these two types of internal voids can also interact during the solidification of a casting. This interaction is termed gas assisted shrink. This porosity has shape characteristics of both shrink and gas porosity.

The size of porosity is another distinguishing feature of the porosity formed in castings. Shrink porosity and gas

porosity can form in macro and micro size voids. Micro porosity is often discussed as voids that form within the mushy interdendritic liquid.[12] Macro porosity is typically discussed within the industry as visible porosity that is compared to quality specifications. Macro porosity may cause rejects within castings with a radiographic (X-ray) inspection or visual inspection after secondary processing, such as machining.[13] A clear definition between micro and macro porosity is lacking and will be discussed.

Micro porosity has been well researched. The stochastic or random nature of micro porosity formation was studied by Atwood.[12] Lee et al.[7] reviewed five different models involving complex simulation of micro porosity and microstructure with random nucleation. Several groups of authors have studied micro porosity formation and distribution in castings with micro computed tomography (CT) equipment.[14–16] Cao et al.[17] and Niu et al.[18] studied porosity formation on the micro scale with vacuum-assisted high pressure die casting. In addition to vacuum, Niu et al.[18] work also studied other injection parameters to see impact on the mechanical properties with micro porosity. Zhang et al.[19] studied micro porosity formation and mechanical properties of both entrapped air and shrinkage. All this work has provided useful insights into how micro porosity forms and the impact it has.

Research on macro porosity is heavily tied to publications on simulations, and it is generally not studied mechanistically like micro porosity. Overall, there is a correlation between porosity results from simulations and where it is found in a casting.[20] Macro porosity can be formed by both shrink and gas porosity. Shrink porosity can be reduced by improving feeding paths in both casting and tool design. Gas porosity is affected by the pour rate, slow shot acceleration, venting, and die lubrication improvements.[2] Since these features of die and process design are well known, there has not been much research on the formation of macro porosity in production environments. This is an oversight because porosity is still a major cause of scrap.[5] Understanding the formation of macro porosity can create a better understanding of inspection and classification of casting defects.

The goal of this work is three-fold. First, a definition will be provided to help distinguish the difference between micro porosity and macro porosity. This definition will be based on an industry perspective within HPDC. Second, the stochastic or random nature of macro porosity will be reviewed with an industrial case study. Simulation software can predict a zone where porosity is likely to form, but it falls short of showing the random formation of voids produced within that zone. Finally, a review will highlight that from first principles macro porosity should be expected to form randomly in unfed liquid pockets. The end results from this work should challenge the accepted analysis of macro porosity in HPDC.

Background on Macro Porosity

The transition dimension between micro porosity and macro porosity has ebbed and flowed between different authors. Huang and Conley[21] said micro porosity was from 0.5 to 1.0 mm, and macro porosity was from 1 to 10 mm. Lee et al.[7] called voids that have a maximum dimension larger than 5 mm as macro porosity. A different approach used by Liang et al.[22] is to call macro porosity anything that can be visibly seen with less than 5X magnification but did not provide a dimension. Zhang et al.[23] used any void less than 300 μm as the transition from macro to micro porosity. Consistency in a definition and the reason for the selected value is lacking from literature. The exact transition dimensions between macro and micro porosity may continue to be challenged; however, definitions should be supported by reasoning. Having a practical definition is needed to provide clarity and consistency within industrial research.

Given the significant impact that macro porosity has on HPDC foundries, a well-conceived definition is needed. The variation seen in the literature is because scope of the definition was too small. Three factors should be considered when defining macro porosity: metallurgical formation mechanism, functional part requirements, and ability to inspect the defect. After considering these factors, the limit of detectability in inspection is the best transition between macro and micro porosity for HPDC.

Metallurgical Formation Mechanism

From a metallurgical perspective, the size where micro porosity transitions to macro porosity is based on the secondary dendrite arm spacing (SDAS). This relationship is due to the different nature of the feeding flow of the bulk liquid versus the feeding in the mushy region between the dendrite arms. In the bulk liquid, the dendrite arms are not present and therefore cannot affect the maximum size of the porosity. This unconstrained macro porosity is formed when the bulk feeding flow is cut off. Dendrites restrict the feeding flow and constrain the maximum size of the porosity, creating micro porosity.[24,25]

Micro porosity size can vary significantly in different casting processes because SDAS is not a constant value for these processes. This is because SDAS is proportional to the cubed root of the cooling rate.[24,26,27] Sand casting and permanent mold castings have a wide range of cooling rates, making a universal definition of interdentric micro porosity in those processes difficult. HPDC cooling rates are different because they are consistently high with an observed SDAS in the range of 10–40 μm.[28] The small value means detecting true micro porosity voids in HPDC is often not industrially practical. This suggests that the definition of macro porosity for HPDC should be driven by

the functional requirements or readily available inspection methods.

Functional Porosity Requirements

Functional casting porosity requirements influence a working definition for macro porosity. After castings are machined, they are inspected for macro porosity on machined surfaces. Acceptance criteria for given surfaces depend on the required function of the casting.[13] Thresholds are sometimes determined by past practices for a given original equipment manufacturer (OEM) and recommendations provided by vendors of assembled components such as piston rings, O-rings, and gaskets. In other cases, thresholds are set by failure points identified in finite element analysis (FEA) for the product. These porosity standards are treated as confidential trade secrets by OEMs; therefore, typical thresholds for specific applications are not published.

The North American Die Casting Association (NADCA) has provided an example of four levels of porosity on exposed machined surfaces in *Die Casting Porosity Guidebook*[1] with a Level 1 porosity being specified as a maximum size of 0.4 mm. Experience by the authors has shown typically that the tightest specifications are a maximum porosity diameter between 0.4 and 0.5 mm (400–500 μm). The threshold for macro porosity would have to be smaller than this minimum acceptable porosity limit to use functional requirements as a meaningful distinction between acceptable and rejectable levels of porosity during inspection.

Inspection Ability

Castings are typically inspected in a raw state with X-ray or computed tomography (CT) equipment or by visual inspection after secondary machining. From an X-ray or CT image standpoint, production intent equipment has a pixel size resolution of 100 μm on castings that can fit up to 400 mm × 400 mm image windows.[29,30] Specialized micro-CT research equipment exists to capture micro porosity resolution of 10–50 μm on parts typically less than 50 mm cube.[14,31] This type of equipment has significant limitations in a production castings environment based on size and time needed to perform analysis. Therefore, the capable range of micro-CT equipment should not be considered in defining an industrial application of macro porosity. The focus should be given to capabilities of industrial, production intent X-ray equipment.

Visual inspection of castings is the next challenge. Visual acuity defines what the human eye is capable of detecting. Snellen eye charts, as typically found at optometrists' offices, were developed based on the studies showing human vision can generally resolve a visual target that represents 5 minutes of an arc. This 5 minutes of an arc is typically referred to as 20/20 vision.[32] The equivalent visual angle of a piece of porosity on a casting is determined based on defect size and surface distance as shown in Eqn. 1. Conversion from degree to minutes of an arc is needed to compare to a Snellen vision chart. Table 1 includes a series of calculated equivalent visual angles for different defect sizes and distances.

$$\text{Tan}\theta = \frac{\text{Defect size}}{\text{Distance from eye}};$$
$$\theta = \arctan\left(\frac{\text{Defect size}}{\text{Distance from eye}}\right) \qquad \text{Eqn. 1}$$

It has been found that human ability to focus on near objects deteriorates with age. Typically, those in their 20s are able to focus down to 150 mm from their eyes. This erodes to 250 mm minimum focal distance as they age.[33] Given that 5 mins of an arc is 20/20 vision,[32] selecting 250 μm threshold between micro and macro porosity provides a realistic size that humans can inspect either without magnification in their youth and with minimal magnification as they age.

Based on the SDAS of HPDC, the functional specifications used to inspect castings, and the ability to detect and identify porosity with X-ray and visual inspection, a threshold of 0.250 mm (250 μm) is a defendable choice for the threshold between micro and macro porosity in HPDC. With a size defined and the reasoning supplied, the porosity that causes rejects in HPDC are macro porosity. The focus can now shift to how this macro porosity forms in production castings and what can be learned to improve the HDPC process.

Experimental Study

A small housing casting, produced on a 900-ton die cast machine out of A362.0 aluminum alloy, as seen in Table 2,

Table 1. Equivalent Visual Angle for Different Defect Sizes and Distances

Equivalent visual angle (minutes of an Arc)

Casting defect size (mm)	Distance from defect (mm)			
	150	250	500	600
0.1	2.29	1.38	0.69	0.57
0.25	5.73	3.44	1.72	1.43
0.5	11.46	6.88	3.44	2.86
0.75	17.19	10.31	5.16	4.30
1	22.92	13.75	6.88	5.73

Si	Fe	Cu	Mn	Ni	Zn	Ti	Sr
10.5–11.5	0.40	0.20	0.25–0.35	0.10	0.10	0.20	0.05–0.07

was selected for this experiment. Previous X-ray audits showed varying levels of porosity within this casting even when process parameters remained consistent. The porosity was located near a semi-circular feature on the side opposite the gating. The porosity level found in this location of the casting does not impact overall part quality based on product testing.

Once the die was brought up to temperature with the typical start-up process, 100 castings were produced at identical process settings. These settings matched the production settings and had no adjustments made for the entire sample run. The castings were pin-stamped with a serial number in the robot extraction cell. With this serial number, all process data are traced to the X-ray images. The castings were completed in just under two hours.

Castings were sawed so the area of interest could be easily X-rayed to provide repeatable images and remove background features non-critical to this study. A sample of the sawed casting is seen in Figure 1. One casting was damaged during the sawing process used to prepare it for the X-ray (sample number 76). Its process information was removed from all analysis. This sample showed no significant difference in process values.

The X-ray equipment used was a Bosello SRE Max with a 225 max KV power rating. Images were registered using open source Fiji imaging software[34] and the selective plane illumination microscopy (SPIM) registration plug-in.[35] The X-ray images were reviewed following ASTM E505 standard[36] to determine porosity cause. Shrink porosity (ASTM Category C) and gas porosity (ASTM Category A) were seen within the castings. The castings were graded with a 1 (best), 2 (moderate), and 3 (worst) score. Figure 2 provides examples of all three gradings.

Results and Analysis

Critical process parameters were collected for all sample castings (n = 99) during the experiment. The data were within typical production variation for the casting. Mean and 95% confidence intervals for these parameters are seen in Table 3. Based on the grading samples on the images, there were 9 samples each identified as Grade 1 (good) and Grade 3 (worst). These parts that represented the extremes of the macro porosity found within the casting were reviewed in detail.

The best castings showed scattered shrink porosity typically 0.2 mm to 0.4 mm thick and up to 1.0 mm long. This porosity was scattered throughout the section in review, with a tendency for it to form furthest way from the gating (part is gated from the left side of the X-ray images). The nine Grade 1 (best) castings can be seen in Figure 3.

The worst castings showed a gas assisted shrink with rounder, but irregular shaped voids, consistent of gas feeding into a shrink porosity. Gas porosity within the

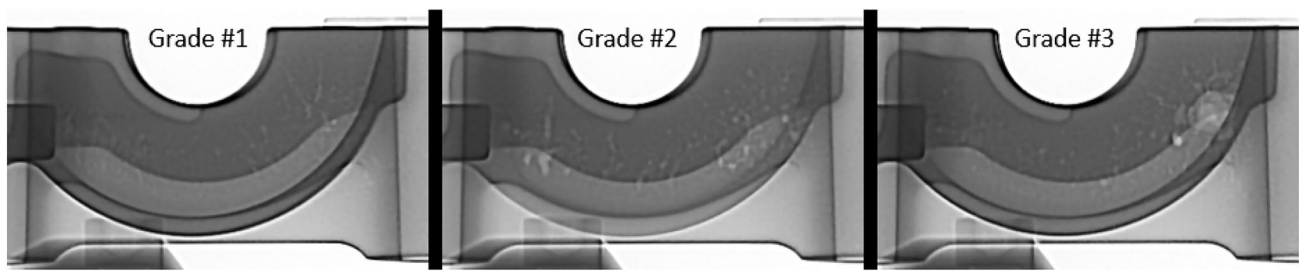Figure 1. Sawed sample casting for X-ray.

Figure 2. Example X-ray gradings 1 through 3.

Table 3. Mean and Confidence Interval of Critical Injection Parameters

	Mean	95% confidence interval for mean	Units
Cycle time	68.0	67.8–68.2	Second
Average slow shot velocity	14.16	14.155–14.165	inches/second
Calculated start of fast shot	14.27	14.266–14.274	Inches
Average fast shot velocity	141.69	141.61–141.77	Inches/second
Intensification pressure	5124.9	5119.0–5130.8	PSI
Intensification squeeze distance	0.174	0.171–0.177	Inches
Biscuit Size	1.69	1.65–1.73	Inches

worst castings grade was typically 3.0 mm to 4.0 mm in diameter. For shrink porosity, the worst castings had 0.4–0.6 mm thick and 5.0–10.0 mm long porosity voids. Overall, the worst of the worst (WOW sample—#43) had an approximate 8.0-mm-diameter void in the casting. The nine worst castings (Grade 3) can be seen in Figure 4.

Shapiro-Wilk normality tests[37] showed the process parameters to be non-normal in the 99 samples. As a result, the Wilcoxon Signed Rank test[38] was performed to compare the samples between the best and worst groupings. Table 4 contains all the individual recorded data for the samples. Table 5 shows the p-values calculated with the Wilcoxon test. None of the critical process parameters showed to be significant.

The results of the experiment have shown that macro porosity formation is random when industry accepted control parameters are held constant in a production environment. The size and distribution of the voids varied significantly throughout the casting run, even though no process settings were changed. When comparing the best and worst samples, the process parameters showed no statistical difference. These parameters remain important to the process, but they do not fully explain the randomness associated with the porosity formation. As will be discussed in the next section, the general location of the porosity formation remained predictable, but the actual macro porosity formation was random. Production controlled processes produce randomly formed porosity. This random macro porosity should challenge many of the

accepted analysis and quality implications of porosity in HPDC.

This experiment could did not determine if the Grade 1 castings were more dense (less porous) than the Grade 3 castings. It simply observes that the levels of macro porosity are higher while no process parameters varied significantly. This leaves open the question of whether the Grade 1 castings traded macro porosity for micro porosity that could not be detected by X-ray. Further study is merited and ongoing.

Part Geometry Impact on Stochastic Macro Porosity Formation

Predicting the morphology of macro porosity is not a useful exercise. Macro porosity is easy to detect with visual inspection on machined surfaces or X-rays. Feeding-based rules have been successfully developed to manage porosity in sand and permanent mold castings. Macro porosity is reduced when an adequately large volume of liquid metal is available to replenish the volumetric contraction of the solidifying metal. The feeding volume must be connected by a liquid path throughout the solidification of the casting's cross sections being fed. From Chorvinov's rule, it can be surmised that thicker sections require more solidification time.[25]

Computer simulations of these feeding rules are effective for identifying where porosity can form, but they fail to properly predict the morphology of the macro porosity.
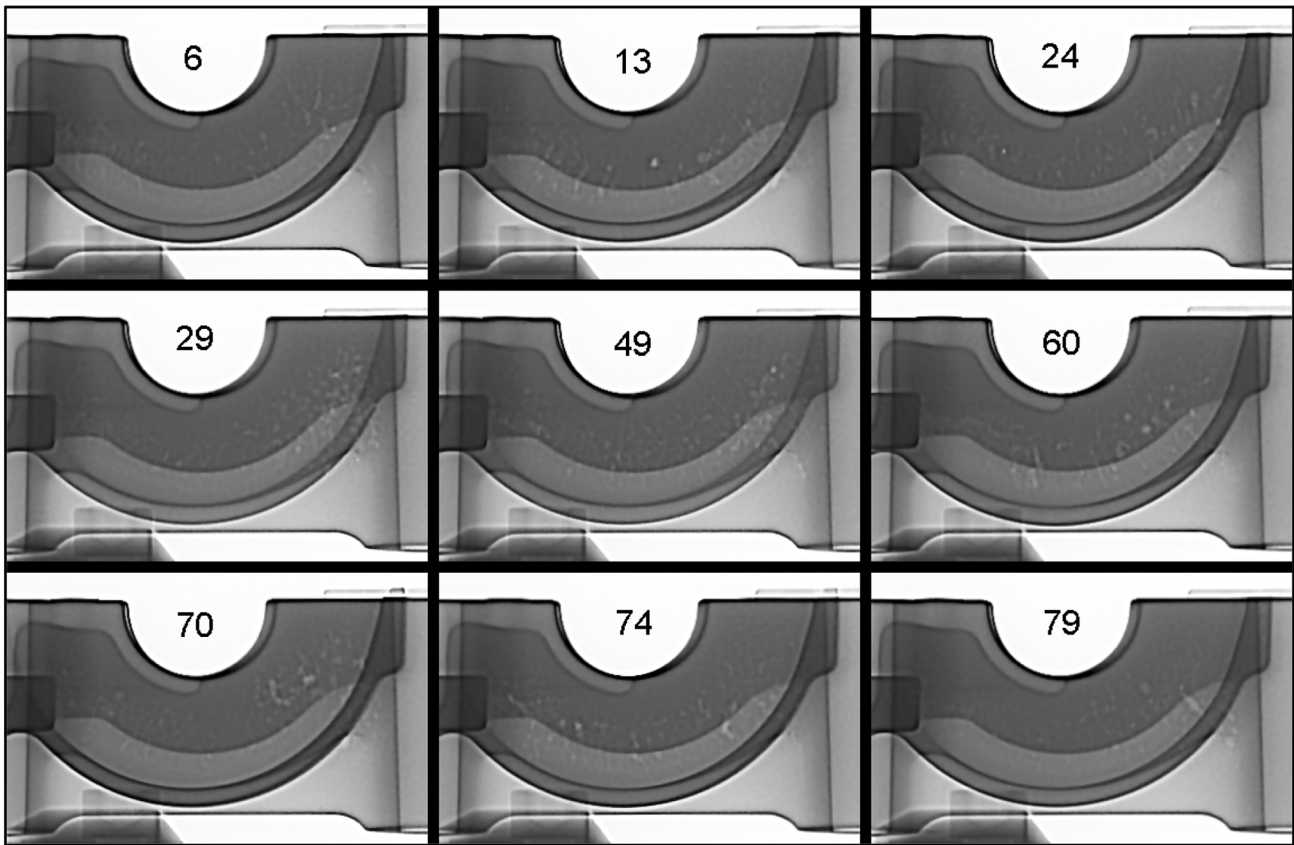
Figure 3. 9 best samples (Grade 1).

MAGMA was used to compare with the experimental results.[39] Six warmup cycles and one production cycle were calculated. Figure 5 shows the predicted porosity zone (a) and the pore volume fraction (b) for the studied casting in the area that was X-rayed. The porosity zone is the predicted hot spot that is the extent of the unfed liquid pocket. Porosity volume fraction is concentrated into two voids that approximate the center of the porosity observed via X-ray. More porosity is predicted on the right-hand side of the image like the experimental results.

Prediction of the macro pore morphology should be nearly impossible. This is because the pressure drop required to homogeneously nucleate porosity is in the giga-Pascal range. Instead, pores require a heterogenous nucleation site such as an oxide bifilm or pre-existing trapped gas pores.[20] Filtering, degassing, venting/vacuum, and good furnace maintenance practices can reduce the number of heterogenous nucleation sites, but they cannot be eliminated. Their occurrence will also be stochastic by nature. Since the nucleation sites are random, the macro pores also must occur randomly. The simulation software can predict these porosity zones but is incapable of showing the randomness of the size and shape of the macro porosity.

Additionally, HPDC feeds exclusively through the gating system into the part. Pressure is applied to enhance feeding, but gate locations are determined by die design and gate removal considerations. A temperature gradient from the thick sections of the casting to the gate cannot be ensured. Resulting unfed pockets of liquid create the macro porosity common to HPDC. Randomly sized and shaped macro porosity voids should form in these trapped pockets, but also the size and shape of the trapped pockets are random because the solidification during filling and time that pressure is applied to the liquid metal after filling is uncertain. Small extension or reduction of feeding will make significant changes to the total porosity due to the rapid solidification from the HPDC process.

Figure 6 plots the liquid volume in the sample area, as seen in Figures 1 and 5, over the entire solidification time of the casting. Feeding is predicted to be cut off to the sample area at 9 seconds after filling, leaving 18.4 cm³ of remaining liquid aluminum. 1.9% of the sample area will contain pores with the assumption that the aluminum will have approximately 6% shrinkage. Increasing or decreasing the feeding time by 0.25 seconds changes the unfed liquid volume by ± 3.5%. These small variations in feeding time can come from a host of uncertainties in the process. For example, cold flakes blocking feeding through the gate, spray variation, initial metal temperature, and other variables can reasonably be assumed to affect the feeding time by 0.25 seconds or more.
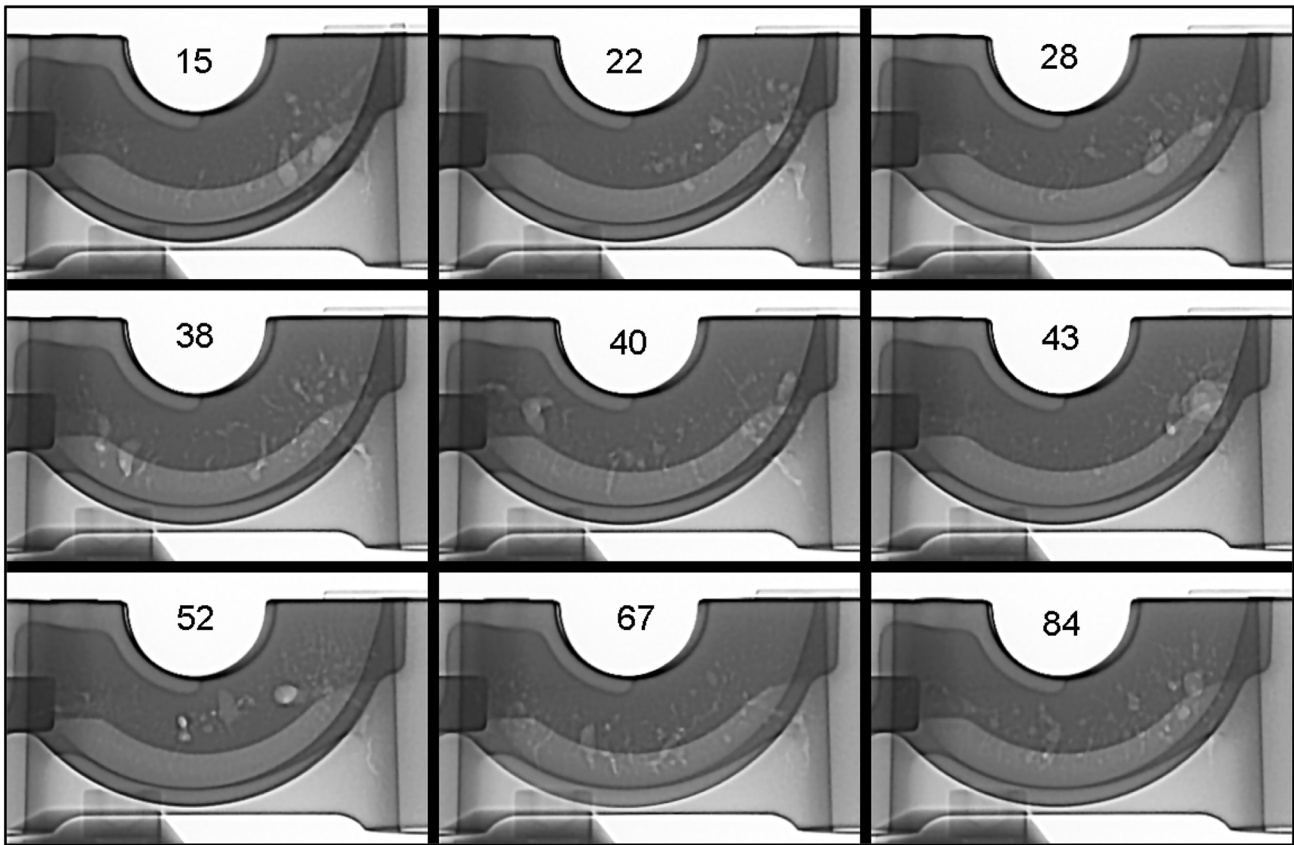
Figure 4. 9 worst samples (Grade 3).

Recommendations

The stochastic nature of macro porosity formation over the course of a normal production run and the inability to predict it precisely should challenge accepted practices within the industry. Cross-functional review of risks associated with the random porosity formation must be considered and identified throughout the casting life cycle. Critical areas that should be rethought include the design of castings, inspection of castings, and casting process optimization.

Design of Castings

Castings free from macro porosity can only exist in a combined effort between casting geometry design and manufacturing process. Manufacturing process will not consistently overcome random macro porosity formation in castings designed with a high probability of porosity. A truly collaborative effort in design for manufacturing (DFM) and finite element analysis (FEA) is required for success. Casting simulation software is accurate at predicting location of macro porosity. However, the random nature of its formation may not guarantee a casting with the worst macro porosity condition is evaluated during functional testing. Casting simulation should be a cornerstone

to the DFM activities on new casting designs. The risks associated with porosity results should not simply be written off to something the process could remove, particularly if inadequate sample sizes are reviewed and tested.

The design validation process should also be reviewed based on this random formation of macro porosity. Larger lots of testing samples should be a focus during the initial production validation process phase. Functional testing should look at both worst case macro porosity formation and other random samples with castings produced with normal production settings. This will require large X-ray studies to help review the amount of macro porosity formation that exist and select the castings that should be functionally tested to ensure product performance.

Inspection of Castings

Because macro porosity forms randomly, variation should be expected during a typical production run. This should cause one to question traditional audit and inspection processes in X-ray and at secondary machining. Better audit sizes can be determined by understanding the probability of uncovering a worst-case macro porosity situation.

Table 4. Injection Parameter Data for Best and Worst Samples

#	Grade	Cycle time (s)	Average slow shot velocity (in/s)	Calc start fast shot (in)	Average fast shot velocity (in/s)	Intens rise time (ms)	Intens pressure (psi)	Intens squeeze distance (in)	Biscuit size (in)
6	1	67.0	14.12	14.30	142.18	69	5096.5	0.157	1.89
13	1	65.8	14.15	14.30	141.34	74	5094	0.167	2.00
24	1	69.3	14.14	14.27	141.65	75	5108.7	0.177	1.79
29	1	67.7	14.18	14.28	141.84	70	5108.7	0.177	1.41
49	1	68.3	14.14	14.28	141.78	71	5123.3	0.157	1.35
60	1	69.0	14.17	14.26	141.87	67	5145.3	0.187	1.67
70	1	68.3	14.15	14.28	141.93	71	5125.8	0.187	1.47
74	1	68.7	14.15	14.27	141.93	72	5164.8	0.177	1.56
79	1	67.6	14.16	14.26	141.58	70	5150.2	0.157	1.59
15	3	67.6	14.13	14.30	142.12	74	5072	0.167	1.91
22	3	67.7	14.15	14.28	141.58	73	5172.2	0.167	1.21
28	3	69.5	14.14	14.29	141.39	70	5116	0.167	1.72
38	3	68.4	14.15	14.28	142.12	73	5101.3	0.167	1.72
40	3	67.8	14.15	14.28	142.12	73	5098.9	0.187	1.71
43	3	66.8	14.17	14.28	142.06	74	5130.6	0.157	1.04
52	3	68.4	14.18	14.27	141.5	71	5223.4	0.128	0.92
67	3	68.5	14.20	14.24	141.14	67	5147.7	0.177	1.76
84	3	68.3	14.21	14.23	142.15	68	5172.2	0.177	1.59

Table 5. Wilcoxon Signed Rank Test p values

	Cycle time	Average slow shot velocity	Calc start fast shot	Average fast shot velocity	Intens rise time	Intens Pressure	Intens squeeze distance	Biscuit size
p value	0.496	0.183	0.233	0.910	0.536	1.0	0.611	0.652

With an exception of some structural automotive parts, in-line X-ray equipment is not typically found in most industrial die casting foundries. The cost of equipment and time to process when compared to the risks of porosity typically makes this an uneconomical process. Instead, audit X-rays are performed on randomly chosen samples during the production run. The number of samples and a defect rate caused by worst-case macro porosity can be used to understand the probability of selecting a sample lot and seeing no defects. The binomial probability function is used to find this probability. Table 6 shows the probability of finding no defects for different defect rates and sample sizes.

Understanding this probability should influence that how troubleshooting is completed within the foundry. As an example, if a casting truly has a 2.5% scrap rate based on the random macro porosity and the X-ray technician randomly pulls 3 castings for inspection, there is 92.7%

chance none of the castings contain that defect. If the defect rate and the process remain constant and the inspection has experience seeing high probability of all good castings, what happens once that inspector finds a defective part? It is slightly better than a coin flip to have a defect occur every two production weeks, based on a three-shift operation. The warning flags in the foundry are sent out, and the troubleshooting begins. Another random sample selected could then show all good parts, and the investigation of "what changed in the process" may occur, wasting resources because the process has not changed, and the sampling was just poor.

Worse yet, someone may take the failed inspection results and change the process to try to "improve it." Now the actual defect rate shifts from 2.5% to some other unknown value. This can lead to a spiral of process changes over the production life of a part, with limited knowledge of what scrap rates are occurring.
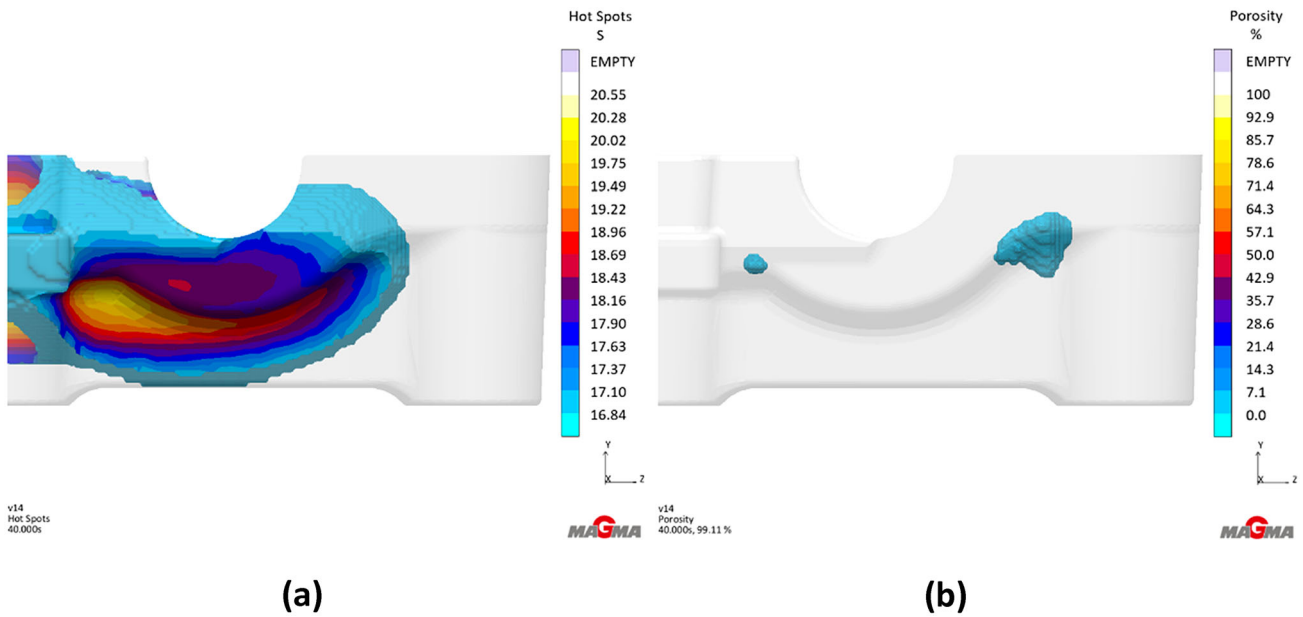
(a)

(b)

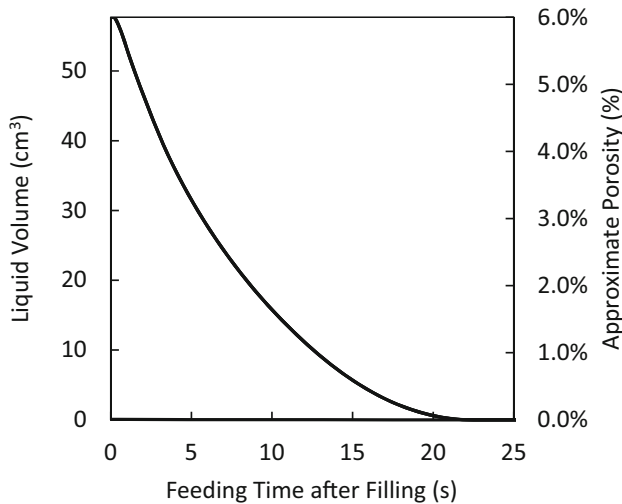*Figure 5. Simulated results of predicted porosity zone.*

Figure 6. Volume of liquid in the sample area as predicted by MAGMA.

By having a good working knowledge of actual scrap rates for given castings based on machining feedback, one can make an educated decision on how to approach the defective audit sample. The Bayes Success-Run Theorem can be used to help determine a lot size given the historical defect rate and the confidence the manufacturing desires.[40]

Casting Process Optimization

The randomness of the macro porosity should cause the industry to review the techniques used for process optimization. An appropriate sample size is needed for any optimization process to ensure the worst-case scenarios are detected in the macro porosity formation. Also, additional process monitoring of the HPDC equipment, beyond the injection system, is needed.

Table 6. Sample Binomial Probabilities

Binomial probability of different defect rates and sample sizes

Defect rate	Number of defects found	Randomly sampled lot size						
		3	5	10	15	30	50	100
1%	0	97.0%	95.1%	90.4%	86.0%	74.0%	60.5%	36.6%
2.5%	0	92.7%	88.1%	77.6%	68.4%	46.8%	28.2%	8.0%
5%	0	85.7%	77.4%	59.9%	46.3%	21.5%	7.7%	0.6%
10%	0	72.9%	59.0%	34.9%	20.6%	4.2%	0.5%	0.0%

Optimization processes are based on feedback from inspection results. With HPDC, that feedback is based on inspection results in either the raw casting state with X-ray images or in a final processed state with a visual inspection for porosity. As discussed previously, lot sizes need to be reviewed and appropriately selected based on historical scrap rates. Without this, samples may not capture the potential worst-case stochastic formation of the macro porosity. This sample size is also pertinent when setting up an optimization design of experiments (DOE). Without the correct sample size, the variation that exists due to the random formation could be missed.

Injection parameters and metal holding temperature are typically the focus of in optimization publications in HPDC.[41–44] This approach is logical given the history and commercially available products for the industry to capture this data. Questions should arise on the focus and priority of these process inputs when significant macro porosity variation occurs. It is clear from simulation that injection parameters can influence predicted zones. This study shows the random formation of porosity in these zones. The injection parameters should remain controlled and monitored; however, data collection on additional process monitoring systems should be prioritized[45] to potentially further reduce this predicted porosity zone. These additional systems could include die temperature,[46] vacuum,[18] and equipment cycle time and performance. Optimization of these additional parameters could reduce the predicted porosity zone. Therefore, the macro porosity that forms in that zone will also be reduced.

Conclusions

High pressure die casting suffers from a porosity problem. By better understanding how macro porosity forms, improvements can be made within the industry. Like micro porosity, macro porosity is randomly formed in HPDC. Casting design, inspection, and optimization processes are all affected by macro porosity. This random macro porosity formation has been shown by an industrial case study and fundamental theory.

Simulation software uses casting geometry and tooling design to predict porosity zones but cannot predict the actual random size and distribution of those voids in the zone. Understanding this stochastic formation should challenge previously accepted practices and improve the comprehension and classification of macro porosity defects in die casting. Specifically, this provides the industry with three areas of further study.

The first area of study is within the industry's process control approach. Injection parameters are the main focus within the industry and academic research for HPDC process control. The conducted experiment shows castings produced with statistically similar injection parameters, cycle time, and biscuit size can produce significantly different levels of porosity as seen in the Grade 1 and Grade 3 examples. This work shows the traditional parameters are not fully capable of reducing the randomness that can exist in the HPDC process. Additional research is needed to understand if other process parameters such as variability in metal cleanliness, furnace temperature, die temperature before die close, spraying, die thermal management, or others could reduce the predicted porosity zone and therefore region where stochastic porosity forms.

The next area to research is the density in the predicted porosity zones between castings. Research has shown that density is not a good predictor of mechanical properties.[47,48] The difference levels of void space visible in the Grade 1 versus Grade 3 X-rays lead to questions regarding the density of the predicted porosity zones. Are the densities of these grade differences the same with different distributions of size of the macro and micro porosity? This is a useful question to have answered as its impact on quality inspection results (acceptable versus scrap casting) and perceived mechanical properties could be misleading to the industry.

From this work, we know there is randomness in the size and shape of macro porosity. This randomness influences classification of defects and process optimization decisions. Misclassification of macro porosity can lead to poor predictions of quality when supervised machine learning algorithms are used. In this case, two significantly different outputs on X-ray images are produced from nearly identical inputs. It becomes impossible for machine learning to find a pattern in what fundamentally becomes noise in the "results" created by random macro porosity formation. Furthermore, sample sizes for optimization studies must be carefully planned based on these random macro porosity formations. Small sample sizes will have a higher probability that the true worst-case macro porosity formation is not seen, thereby providing misleading optimization guidance. These areas are worthy of additional research.

In conclusion, the stochastic nature of macro porosity formation within the prediction porosity zone should challenge the industry to further research HPDC process in production environments. By researching these topics further, the industry will be better positioned to help improve overall HPDC casting design and manufacturing of parts.

Availability of data and material

Not applicable.

Conflict of interests   Research was completed as part of requirements for an author's PhD degree.

Code availability   Not applicable.

REFERENCES

1. J. Brevick, *Die Casting Porosity Guidebook*. North American Die Casting Association, 2008.
2. W.G. Walkington, *Die Casting Defects: Causes and Solutions* (North American Die Casting Association, Rosemont, IL, 1997).
3. D. Twarog, "State of the Industry 2012." North American Die Casting Association, 2012, [Online]. https://www.diecasting.org/archive/dce/212online2.pdf.
4. J. Folk, "U.S. Aluminum Casting Industry - 2019," *Die Casting Engineer*, vol. July 2019, 2019.
5. S. Midson, "Report on the 2014 Die Casting Benchmarking Survey Part 2 of 3: Operations," in *Report on the 2014 Die Casting Benchmarking Survey*, North American Die Casting Association, 2014.
6. S. Viswanathan *et al.*, Eds., "Shrinkage Porosity and Gas Porosity," In: *Casting*, ASM International, 2008, pp. 370–374. https://doi.org/10.31399/asm.hb.v15.a0005222
7. P.D. Lee, A. Chirazi, D. See, Modeling microporosity in aluminum–silicon alloys: a review. J. Light Met. **1**(1), 15–30 (2001). https://doi.org/10.1016/S1471-5317(00)00003-1
8. J. Campbell, *Castings*, 2nd edn. (Butterworth-Heinemann, Oxford, 2003).
9. E. Fiorese, F. Bonollo, G. Timelli, L. Arnberg, E. Gariboldi, New classification of defects and imperfections for aluminum alloy castings. Int. J. Met. **9**(1), 55–66 (2015). https://doi.org/10.1007/BF03355602
10. H.H. Doehler, *Die Casting* (McGraw-Hill Book Company, New York, 1951).
11. *NADCA Product Specification Standards for Die Casting*, 10th Edition. Arlington Heights, IL: North American Die Casting Association, 2018.
12. R. Atwood, "A Combined Cellular Automata and Diffusion Model for the Prediction of Porosity Formation During Solidification," University of London, 2001.
13. *Product Design for Die Casting E-606*, Sixth Edition., vol. E-606. North American Die Casting Association, 2009.
14. I. Brill, B. Kappes, and S. Midson, An Initial Evaluation of CT Scanning for Measuring and Characterizing Porosity in Aluminum Die Castings, Indianapolis, IN, 2018, vol. T18-083. http://www.diecasting.org/archive/transactions/T18-083.pdf
15. M. Weidt, R.A. Hardin, C. Garb, J. Rosc, R. Brunner, C. Beckermann, Prediction of porosity characteristics of aluminium castings based on X-ray CT measurements. Int. J. Cast Met. Res. (2018). https://doi.org/10.1080/13640461.2018.1467105
16. C. Gu, Y. Lu, A.A. Luo, Three-dimensional visualization and quantification of microporosity in aluminum castings by X-ray micro-computed tomography. J. Mater. Sci. Technol. **65**, 99–107 (2021). https://doi.org/10.1016/j.jmst.2020.03.088
17. H. Cao, M. Hao, C. Shen, P. Liang, The influence of different vacuum degree on the porosity and mechanical properties of aluminum die casting. Vacuum **146**, 278–281 (2017). https://doi.org/10.1016/j.vacuum.2017.09.048
18. X.P. Niu, B.H. Hu, I. Pinwill, H. Li, Vacuum assisted high pressure die casting of aluminium alloys. J. Mater. Process. Technol. **105**(1–2), 119–127 (2000). https://doi.org/10.1016/S0924-0136(00)00545-8
19. Y. Zhang, E. Lordan, K. Dou, S. Wang, Z. Fan, Influence of porosity characteristics on the variability in mechanical properties of high pressure die casting (HPDC) AlSi7MgMn alloys. J. Manuf. Process. **56**, 500–509 (2020). https://doi.org/10.1016/j.jmapro.2020.04.071
20. J. A. Dantzig and M. Rappaz, *Solidification*, 1 st. EPFL Press, 2009
21. J. Huang, J.G. Conley, Modeling of microporosity evolution during solidification processes, in *Review of progress in quantitative nondestructive evaluation*. ed. by D.O. Thompson, D.E. Chimenti, (Springer, US, 1998), pp. 1839–1846
22. T. Liang, C. Mobley, N. Tsumagari, *"The Effects of Shot Delay Time on the Microstructures and Mechanical Properties of a Die Cast Aluminum Alloy"*, Presented at the Die Casting Toward The Future (Rosemont, IL, 2002). https://www.diecasting.org/archive/transactions/T02-053.pdf
23. B. Zhang, S.L. Cockcroft, D.M. Maijer, J.D. Zhu, A.B. Phillion, Casting defects in low-pressure die-cast aluminum alloy wheels. JOM **57**(11), 36–43 (2005). https://doi.org/10.1007/s11837-005-0025-1
24. K.D. Carlson, C. Beckermann, Prediction of shrinkage pore volume fraction using a dimensionless Niyama criterion. Metall. Mater. Trans. A **40**(1), 163–175 (2009). https://doi.org/10.1007/s11661-008-9715-y
25. G.K. Sigworth, Shrinkage, feeding and riser design. AFS Trans. **14**(002), 25–36 (2014)
26. M. Shabani, A. Mazahery, Prediction of mechanical properties of cast A356 alloy as a function of microstructure and cooling rate. Arch. Metall. Mater. (2011). https://doi.org/10.2478/v10172-011-0073-1
27. M. Easton, C. Davidson, D. St John, Effect of alloy composition on the dendrite arm spacing of multi-component aluminum alloys. Metall. Mater. Trans. A **41**(6), 1528–1538 (2010). https://doi.org/10.1007/s11661-010-0183-9

28. J. Cho, C. Kim, The relationship between dendrite arm spacing and cooling rate of Al-Si casting alloys in high pressure die casting. Int. Metalcasting **8**(1), 49–55 (2014). https://doi.org/10.1007/BF03355571

29. "SRE MAX," *Bosello High Technology , a ZEISS company*. https://bosello.eu/products/sre-max/. Accessed 29 Dec 2020

30. "Phoenix Vtomex C | 3D CT Scanner (Mini Focus)," *Waygate Technologies*. https://www.bakerhughesds.com/industrial-x-ray-ct-scanners/phoenix-vtomex-c-ct. Accessed 29 Dec 2020

31. "Xradia 610 & 620 Versa." https://www.zeiss.com/microscopy/us/products/x-ray-microscopy/zeiss-xradia-610-and-620-versa.html. Accessed 29 Dec 2020

32. T.J. Schorn, *Improving the Effectiveness of Visual Inspection* (American Foundry Society, Schaumburg, IL USA, 2018).

33. J.F. Koretz, G.H. Handelman, How the human eye focuses. Sci. Am. **259**(1), 92–99 (1988). https://doi.org/10.1038/scientificamerican0788-92

34. J. Schindelin et al., Fiji: an open-source platform for biological-image analysis. Nat. Methods **9**(7), 676–682 (2012). https://doi.org/10.1038/nmeth.2019

35. S. Preibisch, S. Saalfeld, J. Schindelin, P. Tomancak, Software for bead-based registration of selective plane illumination microscopy data. Nat. Methods **7**(6), 418–419 (2010). https://doi.org/10.1038/nmeth0610-418

36. ASTM E505–15, Standard reference radiographs for inspection of aluminum and magnesium die castings E505–15. ASTM International (2015). https://doi.org/10.1520/E0505-15

37. S.S. Shapiro, M.B. Wilk, An analysis of variance test for normality (complete samples). Biometrika **52**, 591–611 (1965)

38. F. Wilcoxon, Individual comparisons by ranking methods. Biom. Bull. **1**(6), 80–83 (1945)

39. *MAGMAsoft*. Kackerstrasse 11, 52072 Aachen, Germany: MAGMA Gmbh, 2019

40. M.R. Brand, An examination of certain Bayesian methods used in reliability analysis. Reliab. Eng. **1**(2), 115–125 (1980). https://doi.org/10.1016/0143-8174(80)90003-7

41. V.D. Tsoukalas, Optimization of porosity formation in AlSi9Cu3 pressure die castings using genetic algorithm analysis. Mater. Des. **29**(10), 2027–2033 (2008). https://doi.org/10.1016/j.matdes.2008.04.016

42. S.G. Lee, A.M. Gokhale, Formation of gas induced shrinkage porosity in Mg-alloy high-pressure die-castings. Scr. Mater. **55**(4), 387–390 (2006). https://doi.org/10.1016/j.scriptamat.2006.04.040

43. Q.-C. Hsu, A.T. Do, Minimum porosity formation in pressure die casting by taguchi method. Math. Probl. Eng. **2013**, 1–9 (2013). https://doi.org/10.1155/2013/920865

44. J. Zheng, Q. Wang, P. Zhao, C. Wu, Optimization of high-pressure die-casting process parameters using artificial neural network. Int. J. Adv. Manuf. Technol. **44**(7–8), 667–674 (2009). https://doi.org/10.1007/s00170-008-1886-6

45. F. Bonollo, N. Gramegna, G. Timelli, High-pressure die-casting: contradictions and challenges. JOM **67**(5), 901–908 (2015). https://doi.org/10.1007/s11837-015-1333-8

46. D. Blondheim Jr., *"Unsupervised Machine Learning and Statistical Anomaly Detection Applied to Thermal Images", Presented at the 2018 NADCA Congress and Exposition* (Indianapolis, IN, 2018). http://www.diecasting.org/archive/transactions/T18-071.pdf

47. C.H. Cáceres, B.I. Selling, Casting defects and the tensile properties of an AlSiMg alloy. Mater. Sci. Eng. A **220**(1–2), 109–116 (1996). https://doi.org/10.1016/S0921-5093(96)10433-0

48. R. Lumley, N. Deeva, M. Gershenzon, An evaluation of quality parameters for high pressure die castings. Int. J. Met. **5**(3), 37–56 (2011). https://doi.org/10.1007/BF03355517